Earthq Eng & Eng Vib (2008) 7:67-75 **DOI**: 10.1007/s11803-008-0768-0

Dynamic performance of angle-steel concrete columns under low cyclic loading-I: Experimental study

Zheng Wenzhong† and Ji Jing§

School of Civil Engineering, Harbin Institute of Technology,No.204 Haihe Road , Harbin 150090 , China

Abstract: This paper describes low cyclic loading testing of nine angle-steel concrete column (ASCC) specimens. In the tests, the influence of the shear-span ratio, axial compression ratio and shear steel plate ratio on the hysteretic behavior, energy dissipation, strength degradation, stiffness degradation, skeleton curve and ductility of the ASCCs is studied. Based on the test results, some conclusions are presented. The *P-Δ* and sectional $M-\phi$ hysteretic models for the ASCCs are presented in a companion paper (Zheng and Ji, 2008).

Keywords: cyclic loading test; ductility; hysteretic model; angle-steel concrete column; shear-span ratio; steel plate stirrup; steel jacketing; seismic retrofitting

1 Introduction

Outer jacketing, a construction technique used to add stories to existing buildings, has become an important issue in urban development in China due to the lack of open land (Zheng *et al.*, 2005). To ensure normal functionality of the original building and to avoid transferring some additional loads to its roof during construction of the outer jacketing, Zheng *et al.*, (2006) proposed a "self-supporting concrete floor during construction" design principle. The principle assumes that the prestressed steel truss carries the self-weight of the frame beams and the additional loads induced during the reconstruction, and the encased prestressed steel-truss concrete composite beams and the outer jacketing columns are connected by fast joints to form an outer jacketing frame. The frame carries additional loads induced by the outer jacketing system during the reconstruction phase. Note that the angle steels of the truss chords in the frame beams take too much space when they pass through the outer jacketing columns, which are used for placing the longitudinal reinforcements in the column, placing the prestressed tendons and the flared pipes in the frame beams, and tensioning and anchoring the prestressed tendons. For this reason, a new construction of the frame structure consisting of encased H-shape steel-prestressed concrete composite beams and angle-steel concrete columns (ASCCs) was presented by Ji Jing *et al*. By hanging the bottom forms below the H steel and then installing the side forms on the bottom forms, the prestressed H-steel can carry the deadweight of the frame beams and construction loads during concreting, and the encased H-steel prestressed concrete composite beams and the outer jacketing columns are connected by fast joints to form an outer jacketing frame, which can bear the newly added load during service.

In ASCCs, the angle steels act as longitudinal reinforcements, and steel plate stirrups welded to the longitudinal angle steels act as reinforcement stirrups. Zhao *et al*. conducted an experiment on nine ASCC specimens with a shear-span ratio of 2.0 under horizontally low cyclic loading, in which the angle steel stirrups or steel plate stirrups were adopted. An analytical expression for evaluating the shear bearing capacity derived from the test was proposed and accepted in engineering practice. However, the test results showed that there were significant pinches in the hysteretic curves of the tested specimens at the moderate and the final stages of loading because of slippage between the angle steels and concrete in the ASCCs. In addition, the energy dissipation and ductility were poor and the stiffness degraded significantly because the shear-span ratio was small. Shi and Bai (2000) performed a similar test on six angle-steel concrete columns specimens, in which the shear-span ratio was 2-3.3 and the reinforcement stirrups were adopted. The test results show that in the specimens that failed

Correspondence to: Zheng Wenzhong, School of Civil Engineering, Harbin Institute of Technology, No.204 Haihe Road, Harbin 150090, China
Tel: 86-451-86283039; Fax: 86-451-86282074
E-mail: zhengwenzhong@hit.edu.cn
†Professor; ‡Graduate Student

Supported by: the New Century Excellent Talents in University Under Grant No.290; Heilongjiang Key Program on Science and Technology Under Grant No.GC04A609 and Harbin Key Program on Science and Technology Under Grant No.2004AA9CS187.

Received September 3, 2007; **Accepted** October 15, 2007

in compression-bending, the hysteretic curves have a plump shape, while in specimens that failed in shear, there were significant pinches in the hysteretic curves because of slippage. In this paper, tests on nine ASCC specimens under horizontally low cyclic loading are described. The specimens have a shear-span ratio (λ) of 3.0, axial compression ratio (n_0) of 0.33 - 0.42 and shear steel plate ratio (ρ_{sv}) of 1.18% - 2.09%, which is defined as the ratio of the steel plate stirrup volume and the volume of core concrete surrounded by angle steels in the length region of the stirrup spacing. The hysteretic behavior, energy dissipation (E), strength degradation (ζ), stiffness degradation (K) and ductility (μ) of the ASCCs are studied and the corresponding hysteretic models are established, which then provide a basis for elastic-plastic dynamic analysis of structures with ASCCs. The *P-Δ* hysteretic model and the sectional $M-\phi$ hysteretic model for the ASCCs are presented in a companion paper (Zheng and Ji, 2008).

2 Description of specimens and test setup

A sketch of the specimens is shown in Fig.1. In all the specimens, the shear-span ratio (λ) is 3, and the cross section is 200mm×200 mm with a clear height of 1200mm. Four ∠30×3 Grade Q345 steel angles are placed in each corner of the specimen as shown in Fig.1, and the corresponding steel ratio is 1.75%. Steel plates are used for shear reinforcement, which is made of Grade Q235 steel plates with thickness of 3 mm. The mechanical properties of the steel are listed in Table 1. The cubic concrete (150mm×150mm×150 mm) compressive strength (f_{cu}) is 56.43 N/mm^2. As shown in Fig. 2, a RC beam (800mm×400mm×300 mm) is fixed at each end of the specimens. Grade HRB 335 and HPB 235 steel bars are used as the longitudinal reinforcements and stirrups, respectively. The main parameters of the specimens are listed in Table 2. 0.76 f_{cu} is regarded as the prismatic concrete compression strength and the contribution of the angle steel to the axial compression ratio for specimens is ignored because it is negligible.

The loading device is shown in Fig. 3. As shown in the figure, the horizontal and vertical loadings are, respectively, the shear force and axial load applied on the specimen, since the four-bar linkage can not support loading in these directions.

3 Test results and discussions

3.1 Failure mode and test process analysis

The results indicated that all the specimens had a ductile compression-bending failure mode. Figure 4 presents a typical failure mode for specimen No. 5. The loading direction and the sign of the column surfaces are shown in Fig. 4(a), where both surfaces perpendicular and parallel to the horizontal loading direction are fronts 1 and 2, and side surfaces 3 and 4, respectively. The specimen was basically at an elastic stage when the horizontal reversible loading was less than 45 kN. Horizontal cracks appeared in the front tensile areas at both ends of the column when the horizontal loading reached 45 kN in the forward direction and 50 kN in the backward direction. As the top displacement of the

Table 1 Mechanical properties of steel

Steel type	Yield strength f_y (MPa)	Ultimate strength f_u (MPa)	Elastic modulus E (MPa)
Angle steel	366	450	1.93×10^5
Steel plate	300	360	2.01×10^5

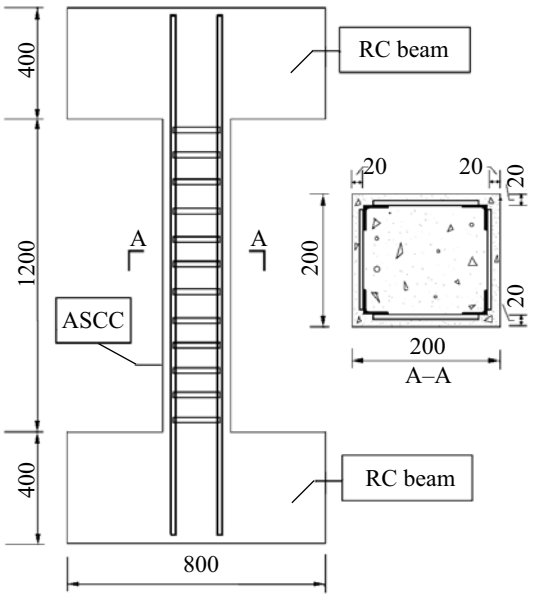

Fig. 1 Sketch of specimen (mm)

Fig. 2 Specimens after demoulding

Table 2 Main parameters of specimens

Specimen No.	Shear-span ratio λ	Axial compression ratio n_0	Shear steel plate ratio ρ_{sv} (%)
1	3	0.33	1.18
2	3	0.33	1.36
3	3	0.33	1.55
4	3	0.37	1.36
5	3	0.37	1.55
6	3	0.37	1.82
7	3	0.42	1.55
8	3	0.42	1.82
9	3	0.42	2.09

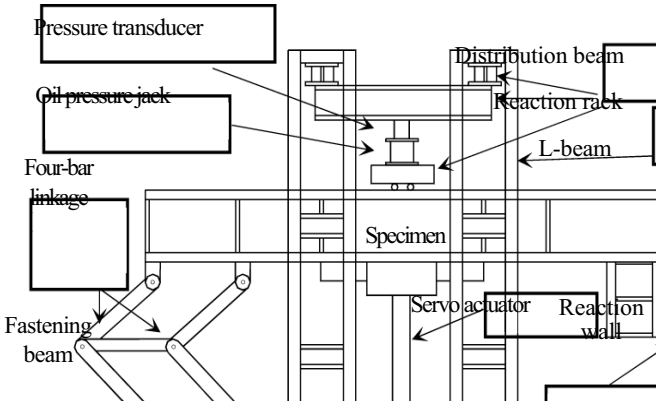

Fig. 3 Sketch of loading device

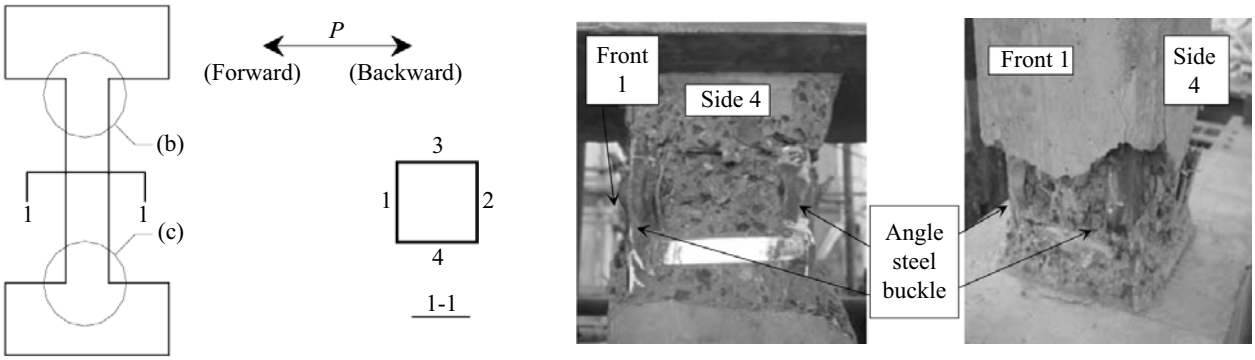

(a) Loading direction and sign of column surfaces (b) Failure at the top (c) Failure at the bottom

Fig. 4 Failure mode of specimen No. 5

column increased, more and more new cracks appeared, existing cracks extended further on the front tensile areas and horizontal cracks appeared on the both sides of both ends of the column at the same time. The concrete at the corners of both ends of the column crushed slightly and parts of the angle steel close to the front tensile areas of both ends yielded when the top displacement of the column reached 9 mm. The concrete at both ends of the column crushed more severely as the top displacement of the column increased. Cracks parallel to the angle steels occurred on both sides of both ends when the top displacement of the column was 18 mm. The concrete at the front compression zones of both ends began to break off gradually as the top displacement of the column increased. The concrete on the fronts and sides of both ends broke off in large areas when the top displacement of the column reached 30 mm. The angle steels and steel plate stirrups were exposed, and the angle steels buckled. Subsequently, the strength of the specimen decreased rapidly until it finally failed.

3.2 Hysteretic curve

The hysteretic curves of load (P)-displacement (Δ) for the nine specimens are shown in Fig. 5. Some characteristics obtained from Fig. 5 are as follows:

(1) The hysteretic loops are plump. After the horizontal load reaches its peak, the hysteretic curves for different cycles are similar under the same controlled displacement. The ductility of the specimens decreases as the axial compression ratio increases.

(2) For specimens with the same axial compression ratio, the greater the shear steel plate ratio, the more plump the hysteretic curve, and the more slowly the stiffness and the strength degrade, and the higher the ductility.

3.3 Energy dissipation behavior

The specimens' capacity for energy dissipation is measured by the areas surrounded by the load-displacement curves as shown in Fig.6 and expressed in terms of the energy dissipation coefficient E (JGJ101-96, 1997) defined as

$$E = \frac{S_{\left(\widehat{ABC}+\widehat{CDA}\right)}}{S_{(\Delta OBE+\Delta ODF)}} \tag{1}$$

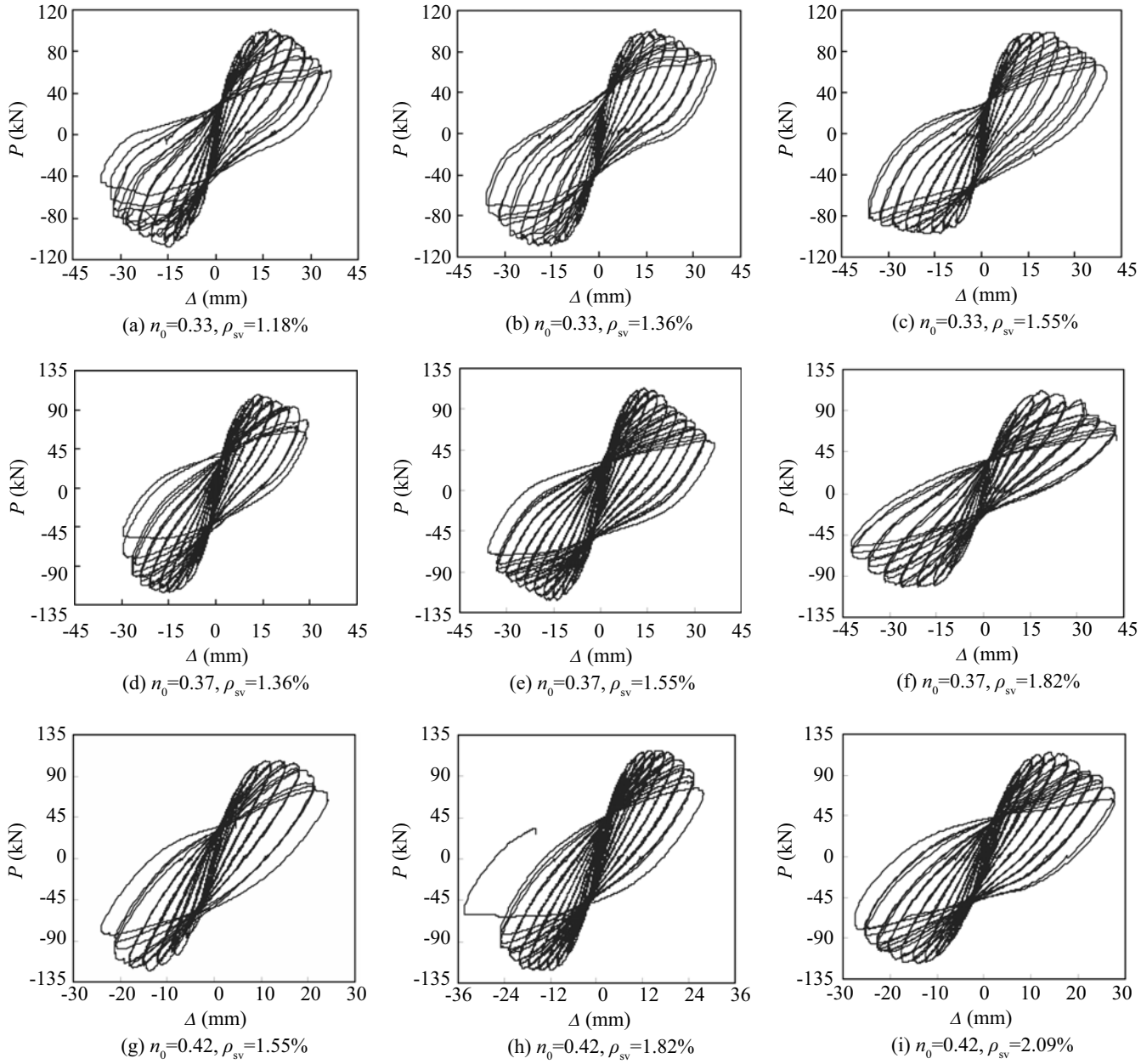

Fig. 5 Hysteretic curves for all specimens

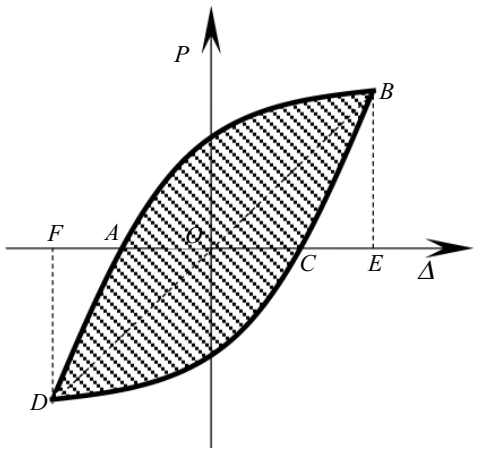

Fig.6 Load-displacement hysteretic curve

The relationship between E and the displacement in the last cycle of all the controlled displacements for all specimens is shown in Fig.7. Note that E increases as the displacement for all specimens increases. For specimens with the same shear steel plate ratio (see Figs. 7 (a), (b) and (c)), E decreases gradually as the axial compression ratio increases. For specimens with the same axial compression ratio (see Figs. 7 (d), (e) and (f)), E increases gradually as the shear steel plate ratio increases.

3.4 Strength degradation

The hysteretic curves of all the specimens show that after the horizontal load reaches its peak, strength decreases as the loading cycles under the same

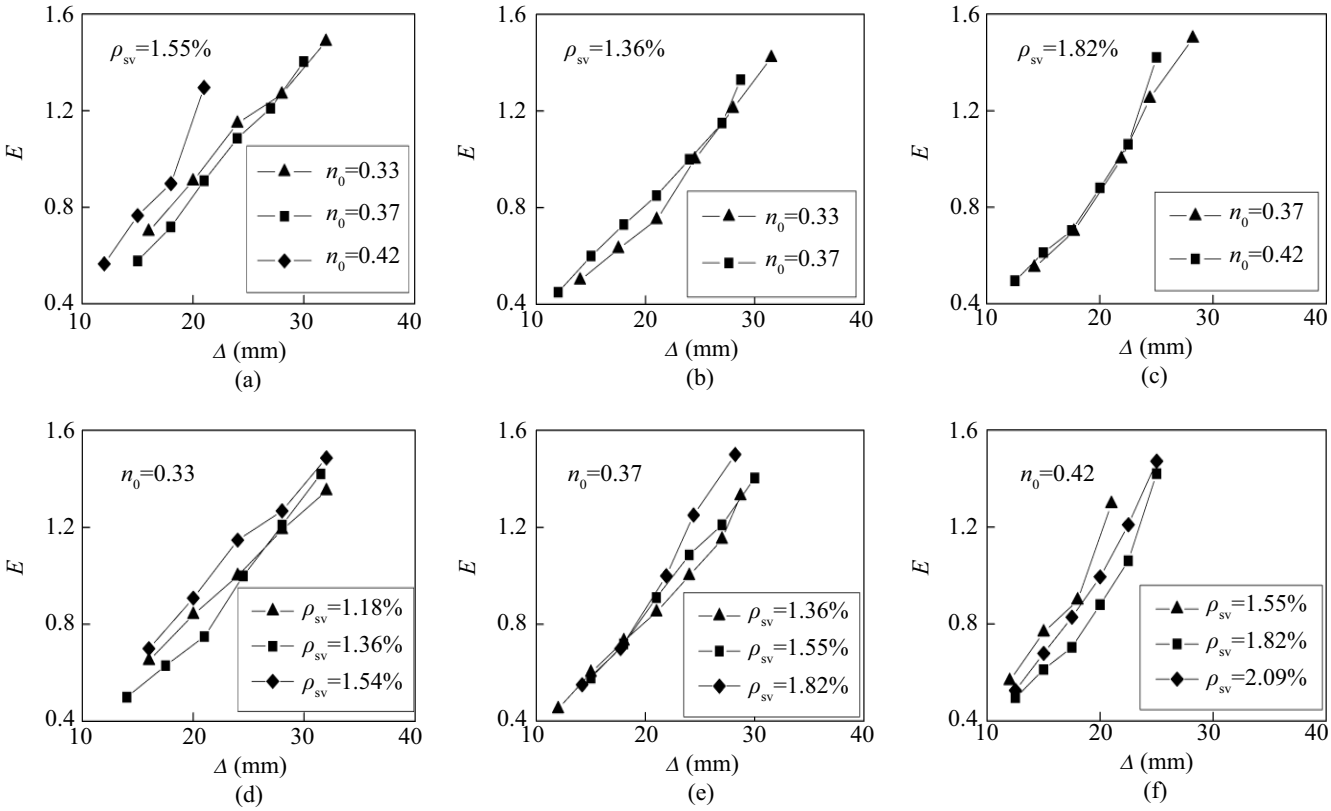

Fig. 7 Energy dissipation coefficient *E* versus displacement for different specimens

controlled displacement increase. This phenomenon is called strength degradation, and is expressed by the strength degradation coefficient ζ_i, defined as the ratio of the peak loads of the *i*th cycle to the first cycle under the same controlled displacements. The relationship between ζ_i and displacements for all specimens is shown in Fig. 8.

For the specimens with the same axial compression ratio, the strength degradation amplitude in the last cycle of the controlled displacement decreases little by little as the shear steel plate ratio increases, as shown in Figs. 8 (a), (b) and (c). For specimens with the same shear steel plate ratio, it increases gradually as the axial compression ratio increases, as shown in Figs. 8 (c), (d) and (e).

3.5 Stiffness degradation

The stiffness of the specimens can be expressed in terms of the secant stiffness K_i (JGJ101-96, 1997), defined as:

$$K_i = \frac{|+P_i| + |-P_i|}{|+\Delta_i| + |-\Delta_i|} \tag{2}$$

where P_i is the peak load in the first cycle under *i*th controlled displacement, and Δ_i is the displacement corresponding to P_i.

Figures 9 (a), (b) and (c) show the relationships between the secant stiffness and the displacement for a given shear steel plate ratio with different axial compression ratios, and Figs. 9 (d), (e) and (f) show the relationships between the secant stiffness and the displacement for a given axial compression ratio with different shear steel plate ratios. Note that in both cases, the secant stiffness decreases as the displacement increases, but the influence of the shear steel plate ratio on the secant stiffness degradation is not very notable.

3.6 Skeleton curve

The skeleton curves for all specimens (see Fig.10) show that the axial compression ratio has some influence on the deformation capacity and strength of the ASCCs. Table 3 shows that the deformation capacity and the ductility are improved by increasing the shear steel plate ratio under the same axial compression ratio.

3.7 Ductility

The ductility is defined as the ratio of the ultimate displacement Δ_u and the yielding displacement Δ_y, i.e.

$$\mu = \Delta_u / \Delta_y \tag{3}$$

In which the yielding displacement Δ_y can be determined by using the energy method (Li, 2005), as

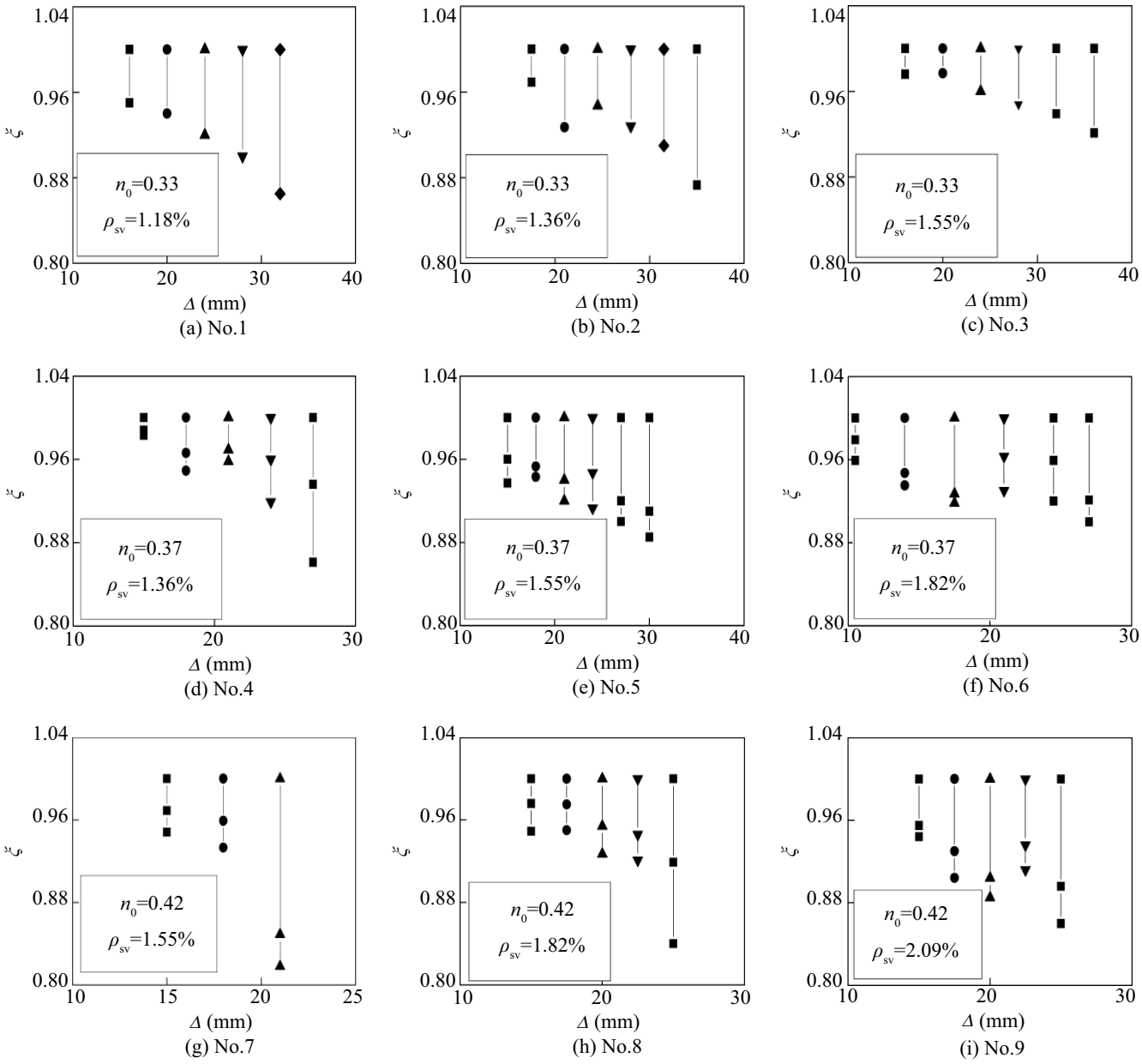

Fig. 8 Strength degradation coefficient ξ versus displacement for different specimens

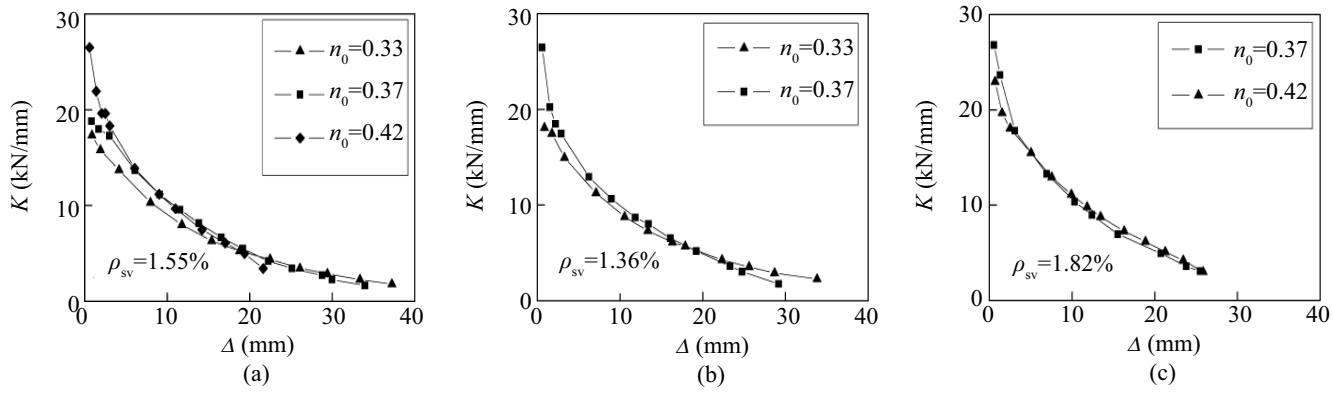

Fig. 9 Secant stiffness coefficient *K* versus displacement for different specimens

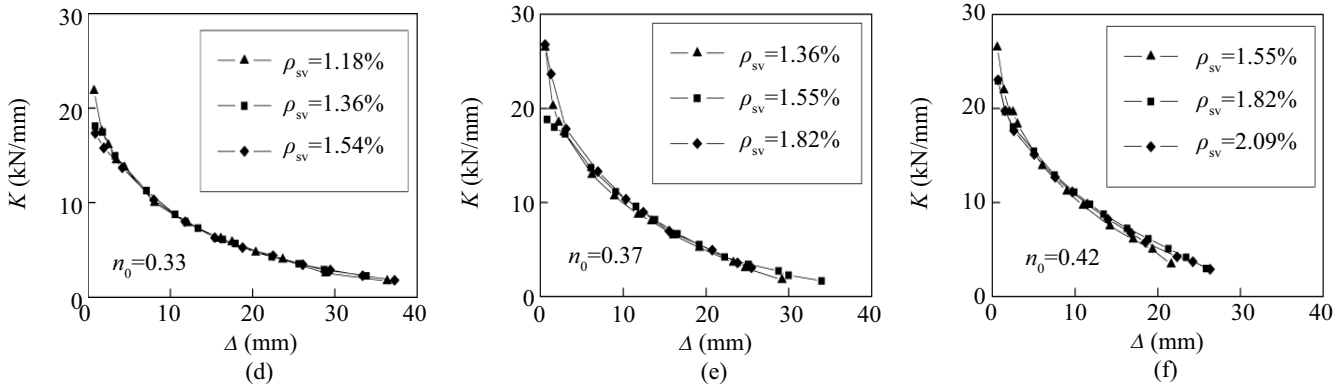

Fig. 9 (Continued)

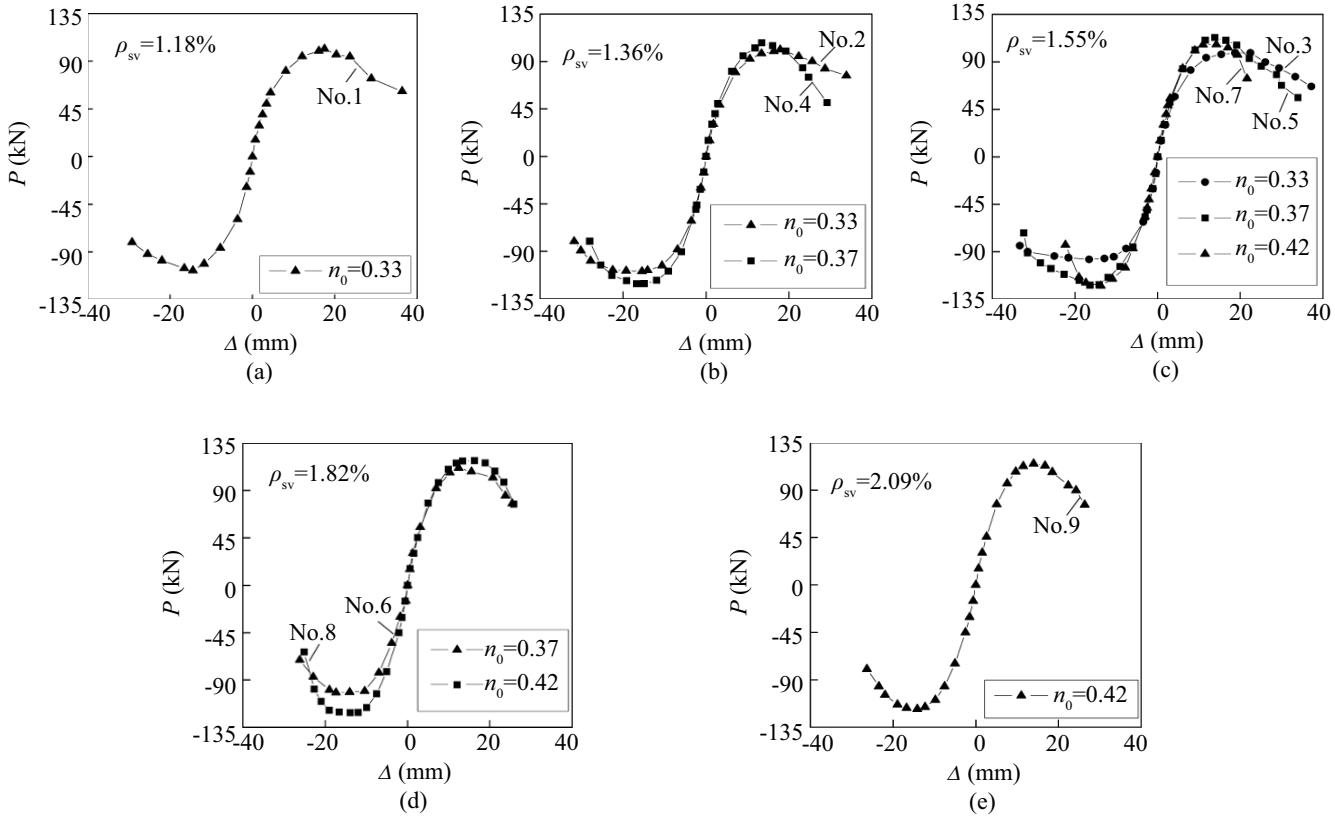

Fig. 10 Skeleton curves for nine specimens

shown in Fig.11, while the ultimate displacement is generally assumed to be the displacement corresponding to 85% of the peak load on the descending segment of the skeleton curve. The calculated ductility coefficients for all specimens tested are listed in Table 3.

Table 3 shows that the axial compression ratio is the main factor affecting the ductility of ASCCs. The ductility coefficients versus the axial compression ratios and shear steel plate ratios are shown in Figs.12 (a) and 12 (b), respectively.

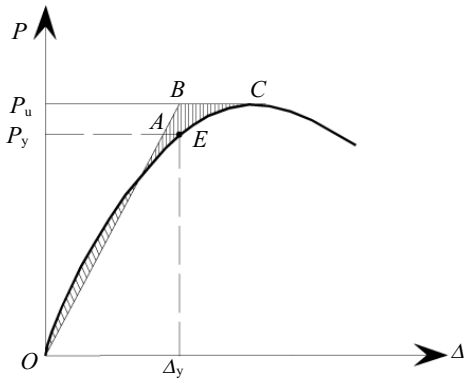

Fig. 11 Yield point calculated using energy method

Table 3 Ductility coefficients for all specimens

No.	Axial compression ratio n_0	Shear steel plate ratio ρ_{sv} (%)	P_y (kN)	Δ_y (mm)	P_u (kN)	Δ_m (mm)	Δ_u (mm)	μ
1	0.33	1.18	77.50	6.89	104.54	15.95	26.03	3.77
2	0.33	1.36	85.00	7.15	105.18	16.66	28.50	3.98
3	0.33	1.55	76.53	6.36	97.89	19.53	31.36	4.93
4	0.37	1.36	91.75	7.03	114.25	15.06	23.55	3.35
5	0.37	1.55	89.00	7.385	121.85	16.38	25.05	3.39
6	0.37	1.82	78.50	5.82	106.66	14.89	22.85	3.92
7	0.42	1.55	97.50	7.48	114.4	13.97	20.15	2.69
8	0.42	1.82	101.00	7.495	119.71	15.11	22.65	3.02
9	0.42	2.09	94.25	7.28	116.35	14.06	22.65	3.11

Note: P_y is horizontal yielding load; P_u and Δ_m are horizontal peak load and corresponding displacement, respectively.

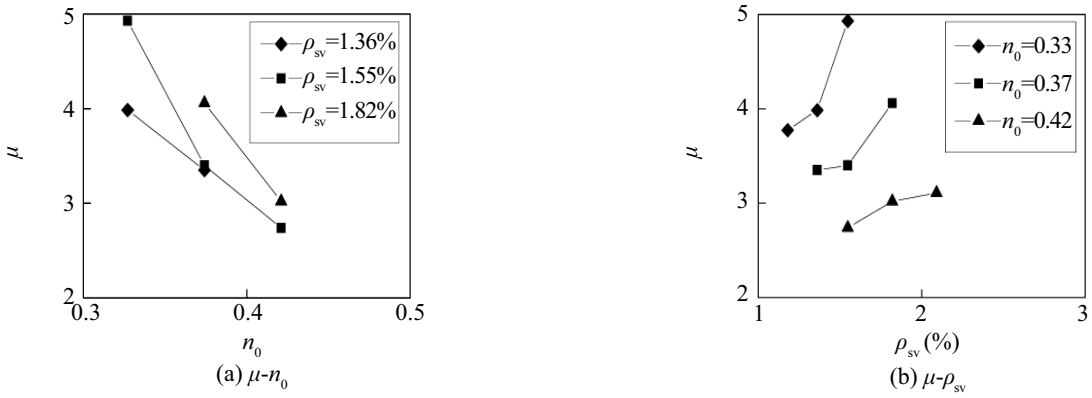

Fig. 12 Ductility coefficient μ versus axial compression ratio n_0 and shear steel plate ratio ρ_{sv} for specimens

4 Concluding remarks

Nine angle-steel concrete column (ASCC) specimens under low cyclic loading were tested. They all had steel plate stirrups and a shear-span ratio of 3. The failure mode, hysteretic curves, energy dissipation (E), strength degradation (ζ), stiffness degradation (K) and ductility (μ) observed in the tests are presented in this paper. The following conclusions can be drawn.

(1) The hysteretic curves of the ASCCs are plump and there is no significant pinch phenomenon or severe decline after the peak load;

(2) As the axial compression ratio increases, both the energy dissipation and ductility decrease while the strength degradation amplitude and bearing capacity increase and the stiffness degrades more rapidly;

(3) As the shear steel plate ratio increases, both the energy dissipation and ductility increase while the strength degradation amplitude decreases and the stiffness degradation remains nearly the same.

In summary, the ASCC shows good dynamic performance under cyclic loading. Note that in addition to using ASCCs for outer jacketing reconstruction when adding stories to existing buildings, they can also be used in the seismic retrofit of existing structures. Compared to steel jacketed columns that are widely used to retrofit bridges (Shinozuka et al., 2002), ASCCs may have less of a lateral confinement effect on the core concrete, but could provide better strength of the cover concrete outside the outer jacketing steel. Moreover, if more closing steel plate stirrups are adopted in the end region of the ASCC as the reinforcement stirrups in the common concrete column, their dynamic performance may be further improved.

Acknowledgements

The study described in this paper was supported by the New Century Excellent Talents in University (Grant No.290), Heilongjiang Key Program on Science and Technology (Grant No.GC04A609) and Harbin Key Program on Science and Technology (Grant No.2004AA9CS187). This support is gratefully acknowledged.

References

JGJ101-96 (1997), *Specification of Testing Methods for Earthquake Resistant Building*, Beijing: China

Architecture Industry Press. (in Chinese)

Li JH (2005), "Study on the Performance of Steel Reinforced High-strength Concrete Columns Under Low Cyclic Reversed Loading," *Ph.D. thesis*, Xi'an, Xi'an University of Architecture and Technology.

Shi J and Bai GL (2000),"An Experimental Study on Restoring Force Characteristics of Lattice Type Steel Reinforced Concrete Frame Columns," *Journal of Xi an Highway University*, **4**(20): 94-97. (in Chinese)

Shinozuka M, Kim Sang-Hoon, Kushiyama Shigeru and Yi Jin-Hak (2002), "Fragility Curves of Concrete Bridges Retrofittd\ed by Column Jacketing," *Earthquake Engineering and Engineering Vibration*, **1**(2): 195-205.

Zheng WZ and Ji Jing (2008), "Dynamic Performance of Angle-steel Concrete Columns Under Low Cyclic Loading-II: Parametric study," *Earthquake Engineering and Engineering Vibration*. (Accepted for publication)

Zheng WZ, Liu T and TAN J (2006), "Design Methods and Construction Techniques for the Outer-jacketing Structure Reconstruction (Extension) Project of Suifenhe Qingyun Market," *Civil Engineering Journal*, **11**(39): 68-76. (in Chinese)

Zheng WZ, WANG Y, Liu T and TAN J (2005), "Thoughts and Understanding of Remodelling of Adding Storeys Around Existing Building," *Industrial Construction*, **4**(35): 1-5. (in Chinese)